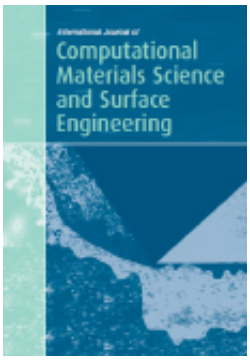

International Journal of Computational Materials Science and Surface Engineering

ISSN online: 1753-3473 - ISSN print: 1753-3465
https://www.inderscience.com/ijcmsse

Improving engine's lubrication based on optimised partial micro-textures

Jili Zha, Vanliem Nguyen, Tianfeng Ye

DOI: 10.1504/IJCMSSE.2023.10058111

Article History:

Received:	11 February 2023
Last revised:	14 February 2023
Accepted:	26 June 2023
Published online:	08 January 2024

Improving engine's lubrication based on optimised partial micro-textures

Jili Zha and Vanliem Nguyen*

School of Mechanical and Electrical Engineering,
Hubei Key Laboratory of Intelligent Conveying Technology and Device,
Hubei Polytechnic University,
Huangshi, 435003, China
Email: zhajili.hbpu@gmail.com
Email: xuanliem712@gmail.com
*Corresponding author

Tianfeng Ye

College of Electrical and Electronic Information Engineering,
Hubei Polytechnic University,
Huangshi, 435003, China
Email: yetianfeng.hbpu@gmail.com

Abstract: The partial textures (PT) used by spherical textures (ST), circular cylinder textures (CCT), conical textures, wedge-shaped textures (WST), and square cylinder textures are designed on the crankpin-bearing (CB) to improve the lubrication of an engine. Based on the lubrication model of CB, the effect of PT's dimension/distribution densities on the lubrication performance is analysed. Radius and depth of PT are then optimised to maximise lubrication of an engine. This study's objective is the decrease F_f (CB's friction force) and increase p (oil film's pressure). Results indicate that engine's lubrication using PT is better than using full textures. Also, the lubrication in an engine using ST is also better than using other PT. Especially, with ST optimised, both maximum p and F_f are ameliorated by 8% and 25% in comparison with full textures. Consequently, CB's bearing surface designed by optimised ST should be applied to further improve engine's lubrication.

Keywords: lubrication model; crankpin bearing; spherical textures; conical textures; square cylinder textures; wedge shaped textures; optimisation algorithm; lubrication performance.

Reference to this paper should be made as follows: Zha, J., Nguyen, V. and Ye, T. (2023) 'Improving engine's lubrication based on optimised partial micro-textures', *Int. J. Computational Materials Science and Surface Engineering*, Vol. 11, Nos. 3/4, pp.233–252.

Biographical notes: Jili Zha is an Ass. Prof. Doctor and Lecturer at School of Mechanical and Electrical Engineering, Hubei Polytechnic University. His current research interests include vehicle and mechanical dynamics, optimal design, engineering materials, micro structure.

Vanliem Nguyen is a doctor and works at Hubei Key Laboratory of Intelligent Conveying Technology and Device, Hubei Polytechnic University. His current research interests include vehicle dynamics, vibration and optimisation control, and lubrication in the engine.

Tianfeng Ye is a Lecturer at Hubei Polytechnic University. His current research interests include vehicle and mechanical dynamics, and engineering materials.

1 Introduction

In order to optimise the working performance in journal bearings, their dynamics coefficients and dimensions influenced on the lubrication performance had been studied and analysed in the existing research. The bearing and shaft surfaces were then investigated and embedded by the micro-textures for enhancing the thickness and pressure of the oil film in the journal bearings' working process (Kim et al., 2014; Liu and Ye, 2021; Ni et al., 2022; Zhang et al., 2022). The lubrication in journal bearings was then significantly ameliorated in comparison without the micro-textures. The influence of micro-textures' shape and dimension on the journal bearings' pressure distribution as well as lubrication efficiency was also evaluated to optimum journal bearings' lubrication (Sinanoğlu et al., 2005; Mourier et al., 2010; Bolutife et al., 2015; Arulbrittoraj et al., 2020). To assess in detail the journal bearings' lubrication using micro-textures designed on journal bearings, the various micro-textures used by oval textures, spherical textures, circular-square textures (CST), and circular cylinder textures (CCT) had been investigated, respectively (Guzek et al., 2013; Michalec et al., 2021). Then, the experiment of the spherical textures and square-cylinder textures was also done to assess the actual lubrication performance of the journal bearings using the micro-textures (Papadopoulos et al., 2011; Fouflias et al., 2017). Result indicated that the structures of spherical textures or square cylinder textures could better ameliorate the lubrication in journal bearings in comparison with other shapes of the micro-texture.

From the lubrication performance of spherical textures or square cylinder textures investigated and applied to journal bearings in existing investigations, the bearing surface of the crankpin bearing was then studied and added by the spherical textures to decrease the friction and improve the engine's lubrication (Wang et al., 2021; Hua et al., 2022). Then, the optimisation of design parameters of spherical textures was done to further ameliorate the engine's lubrication (Dobrica et al., 2010; Nguyen et al., 2021; Hua et al., 2022; Jain and Parashar, 2022). The investigation result indicated that the friction of the crankpin bearing was significantly reduced while the lubrication of the engine was significantly changed and enhanced by using spherical textures compared to without spherical textures. However, in the studies of the bearing surface of engine's crankpin bearing using micro-textures, researchers also noted that both the friction force and pressure of the oil film in crankpin bearing was only improved when the minimum value of the oil film thickness was smaller than 10 μm and this mainly appeared at the crankpin bearing's mixed lubrication. Conversely, the studies of Kim et al. (2014) and Zhang et al. (2022) showed that the friction force and pressure of the oil film in the journal bearings were insignificantly ameliorated by using the micro-textures when the minimum

thickness of the oil film was more than 10 μm. This mainly appeared at the hydrodynamic-lubrication region in journal bearings' surfaces. Based on these investigation results, the partial textures should be researched and embedded at the mixed-lubrication region in crankpin bearings for ameliorating the engine's lubrication. This not only improves the engine's lubrication but also is technologically simple compared to micro-textures added throughout the crankpin bearing's surface. But this problem has not been investigated yet. Moreover, the evaluation of the crankpin bearing's lubrication using both structures of conical textures and wedge-shaped textures (WST) has not also been researched yet.

To solve these existing issues in the lubrication of engine's crankpin bearing using micro-textures, at the mixed-lubrication range of crankpin bearing, the surface of the bearing designed by partial textures using spherical textures (ST), CST, CCT, conical textures (CT), or WST is investigated in this paper. To assess the crankpin bearing's lubrication using various partial textures, based on the lubrication model of engine's crankpin bearing and model of partial textures established, all the shapes, depths, and dimensions of partial textures are then simulated and analysed under the different dynamic load of the engine. Then, these parameters are also optimised for further ameliorating engine's lubrication via two assessing indicators in the pressure (p) of the oil film and friction force (F_f) of crankpin bearing.

The novelty of this study is summarised as follows:

1 The partial textures are proposed and designed on the mixed-lubrication region of the bearing surface in an engine's crankpin bearing to maximise lubrication of an engine.

2 The lubrication performance in an engine's crankpin bearing using different structures of the partial textures and the influence of their design parameters are studied and evaluated, respectively.

3 To further ameliorate an engine's lubrication, the radius and depth of spherical textures are also optimised via a multiobjective optimisation method.

2 Crankpin-bearing's hydrodynamic lubrication model

2.1 Modelling of crankpin bearing's lubrication and partial textures' design

In order to assess the partial textures' efficiency on ameliorating the lubrication in the crankpin bearing under the impact of the F_c (slider crank mechanism's dynamic load), a 3D structure and lubrication model of crankpin bearing embedded by partial textures on its bearing surface have been built in Figure 1(a) and (b). Besides, in order to calculate both values of the thickness and pressure of the oil film in crankpin bearing, the model of the Cartesian counterpart (Shen and Khonsari, 2015, Ni et al., 2022) was also used for computing the lubrication parameters in engine's crankpin bearing as well as designing partial textures in crankpin bearing's bearing surface, as illustrated in the same Figure 1(b).

Under the influence of the dynamics load F_c impacting on engine's crankpin bearing, the maximum pressure and minimum thickness of the oil film were reached at a range of ψ from $\pi/2$ to π. This was the mixed-lubrication region of crankpin bearing and it greatly affected the engine's lubrication performance (Dobrica et al., 2010; Michalec et al.,

2021). Thereby, partial textures need to be added on the bearing surface at this range for ameliorating the engine's lubrication, as illustrated in the same Figure 1(b).

Figure 1 Structure and lubrication model of the engine: (a) 3D structure of engine's slider crank mechanism and (b) lubrication model of crankpin bearing added by micro-textures (see online version for colours)

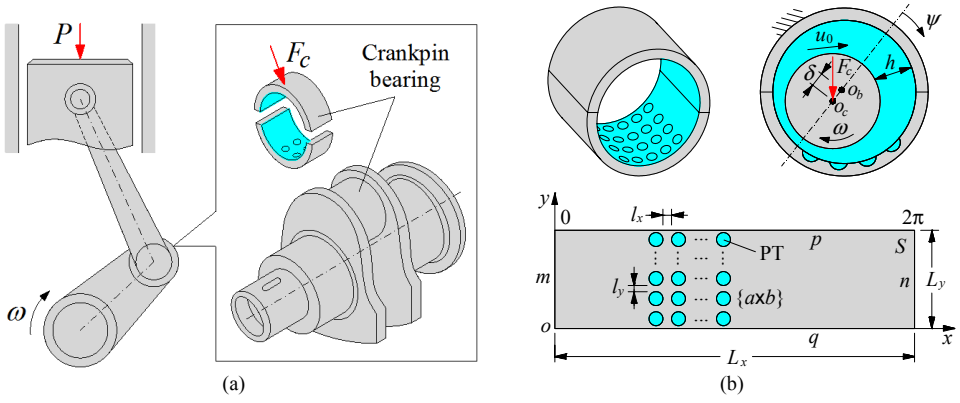

Where P is the pressure in the combustion chamber acts on the top of the piston; F_c is the dynamic load of an engine's slider crank mechanism acting on crankpin bearing; ω is the angular speed of the engine's crankshaft; ψ is the crankpin bearing's angular coordinate; δ is the eccentricity of the bearing and crankpin; u_0 is the relative speed of two crankpin and bearing surfaces; h is the thickness of the oil film used to lubricate between crankpin and bearing surfaces; S is crankpin bearing's lubrication area; $\{a \times b\}$ is the partial textures' matrix; $\{L_x$ and $L_y\}$ and $\{l_x$ and $l_y\}$ are dimensions of the bearing surface and partial textures in the x and y direction; m and n are the crankpin bearing's initial and final pressure at $\psi = 0$ and $\psi = 2\pi$; p and q are the left and right pressures at 0 and L_y of the crankpin bearing, respectively.

In addition, the partial textures' various structures applied by spherical textures, CCT, conical textures, square cylinder textures, and WST are also researched to evaluate their performance in ameliorating the engine's lubrication. Their structures are shown in Figure 2. Herein, h_{oil} is the thickness of the oil film existing between the crankpin and bearing surfaces; $h_{textures}$ is the thickness of the oil film (or depth of designed micro-textures); R is the radius of spherical textures, CCT, and conical textures while l_t is the rectangle's length of the square cylinder textures and WST, respectively.

In order to ensure the lubrication of crankpin bearing, a small gap always exists in crankpin bearing and it is written as $\kappa = R_{bearing} - R_{crankpin}$. Herein, $R_{crankpin}$ and $R_{bearing}$ are the radius of the crankpin and bearing. Therefore, under the movement of the crankpin in the bearing, an eccentric ratio between the bearing and crankpin exists and it is defined by $\zeta = \delta/\kappa$. Based on this ratio, the oil film thickness in an engine's crankpin bearing could be computed by:

$$h_{oil} = (\zeta \cos\gamma + 1)\kappa \tag{1}$$

Based on the crankpin bearing's oil film thickness calculated in equation (1), the actual oil film thickness of the crankpin bearing embedded by the $h_{textures}$ of the partial textures is expressed as follows:

$$h = h_{oil} + h_{textures} = (\zeta \cos\gamma + 1)\kappa + h_{textures} \tag{2}$$

In order to assess the various textures' effect on an engine's lubrication, the mathematical equations of all the spherical textures, CCT, conical textures, square cylinder textures, and WST need to be determined. From the distribution of different micro-textures described in Figure 1(b), their distribution equations are calculated by:

$$L_x = 4a(l_x + \Pi) \text{ and } L_y = b(l_y + \Pi), \quad \Pi = \begin{cases} 2R & \text{with ST, CCT, and CT} \\ l_t & \text{with SCT and WST} \end{cases} \tag{3}$$

With the structure of the spherical textures, CCT, and conical textures added in the crankpin bearing's bearing surface, their shape and depth were determined by (Zhang et al., 2022):

$$h = \begin{cases} h_{oil} + h_{textures} + H_{textures} & \text{with } R_{textures} < R \\ h_{oil} & \text{with } R_{textures} > R \end{cases} \tag{4}$$
$$R^2 = (x - x_i)^2 + (y - y_j)^2$$

where $H_{textures} = \sqrt{(R^2 + h_{textures}^2)^2 / 4h_{textures}^2 - R_{textures}^2} - (R^2 + h_{textures}^2) / 2h_{textures}$.

With the structure of the square cylinder textures and WST added in the crankpin bearing's bearing surface, their shape and depth were determined by

$$h = \begin{cases} h_{oil} + h_{textures} & \text{with } |x - x_i| < 0.5l_t \\ h_{oil} & \text{with } |x - x_i| \geq 0.5l_t \end{cases} \tag{5}$$

where $h_{textures}$ is a constant with the micro-textures of circular cylinder and square cylinder textures while $h_{textures}$ with the spherical textures, conical textures, and WST is changed and determined as in equation (6); x_i and y_j are two coordinates in each micro-texture in the x and y direction and they are computed as in equation (7).

$$h_{textures} = \begin{cases} \sin\delta(1 - \cos\delta)R & \text{with ST} \\ R\tan\delta & \text{with CT} \\ 0.5l_t \tan\delta & \text{with WST} \end{cases} \tag{6}$$

$$x_i = \frac{L_x + (2i - 1)(2l_x + R)}{4} \text{ and } y_j = \frac{(2j - 1)(2l_y + R)}{4} \tag{7}$$

where $a \geq i \geq 1$ and $b \geq j \geq 1$.

From the mathematical equations of shape, depth, and distribution of all the various micro-textures calculated in equations (1)–(7), these mathematical equations have been used for simulating and assessing the lubrication in an engine's crankpin bearing using different textures.

Figure 2 Structure of the partial micro-textures designed on an engine's crankpin bearing: (a) ST; (b) CCT; (c) CT; (d) SCT and (e) WST (see online version for colours)

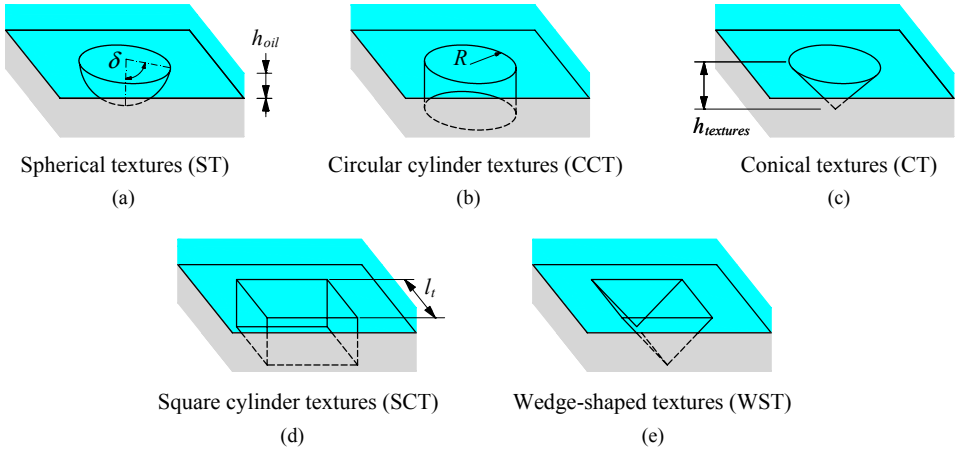

Spherical textures (ST) (a) | Circular cylinder textures (CCT) (b) | Conical textures (CT) (c)

Square cylinder textures (SCT) (d) | Wedge-shaped textures (WST) (e)

2.2 *Reynolds equation for hydrodynamic lubrication with its application*

To evaluate an engine's lubrication using micro-textures, the lubrication equations of the engine's crankpin bearing and micro-textures need to be determined. Based on the actual working condition of the engine's crankpin bearing, it is assumed that the bearing has been fixed in the x and y direction while the crankpin is moved with the speed u_0 in x direction. Therefore, the boundary speed of the oil film on the crankpin and bearing surface is calculated as:

$$\begin{cases} u = 0 & \text{at } z = 0 \\ u = u_0 & \text{at } z = h \end{cases} \tag{8}$$

In the actual condition, the inertia of the oil film is small and ignored in the computation process. In addition, the density and viscosity of the oil film in an engine's crankpin bearing are also defined as unchanged during work. Therefore, the oil film pressures in the x and y direction were calculated as (Nguyen et al., 2021; Wang et al., 2021):

$$\frac{\partial p}{\partial x} = \frac{\partial \tau}{\partial z} = \frac{\partial}{\partial z}\left(\frac{\eta \partial u}{\partial z}\right) \quad \text{and} \quad \frac{\partial p}{\partial y} = \frac{\partial \tau}{\partial z} = \frac{\partial}{\partial z}\left(\frac{\eta \partial v}{\partial z}\right) \tag{9}$$

where η is the dynamics viscosity of the oil film.

From two initial conditions of the oil film's speed in equations (8), (9) is then derivative twice in the z direction to obtain the speed equations of the oil film. The speed equations in two directions of x and y have been written by:

$$u = \frac{1}{2\eta}\frac{\partial p}{\partial x}(z^2 - hz) + u_0 z h^{-1} \quad \text{and} \quad v = \frac{1}{2\eta}\frac{\partial p}{\partial y}(z^2 - hz) \tag{10}$$

Based on the calculation equation of the fluid continuity equation, its equation is given by (Patir and Cheng, 1978):

$$\frac{\partial(\rho u)}{\partial x}+\frac{\partial(\rho v)}{\partial y}=0 \tag{11}$$

where u and v are the velocity of the oil film in the x and y direction; ρ is the oil density in the journal bearing.

By replacing the velocity values of u and v in equation (10) into equation (11) and mathematical transformation of equation (11), the Reynolds equation of equation (11) is obtained as follows (Patir and Cheng, 1978, 1979):

$$\frac{\partial}{\partial x}\left(\phi_x h^3\frac{\partial p}{\partial x}\right)+\frac{\partial}{\partial y}\left(\phi_y h^3\frac{\partial p}{\partial y}\right)=6\eta\left[u_0\left(\frac{\partial h}{\partial x}+\varsigma\frac{\partial \phi_s}{\partial x}\right)+2\frac{\partial h}{\partial \phi}\right] \tag{12}$$

Equation (12) is the lubrication equation of the crankpin bearing. To solve this equation, its non-dimension form is written as (Zhang et al., 2022; Xu et al., 2022):

$$\chi^2\frac{\partial}{\partial X}\left(\phi_x H^3\frac{\partial P}{\partial X}\right)+\frac{\partial}{\partial Y}\left(\phi_y H^3\frac{\partial P}{\partial Y}\right)=\Gamma\left[\frac{u_0\phi_0}{L_x}\left(\frac{\partial H}{\partial X}+\frac{\varsigma}{\kappa}\frac{\partial \phi_s}{\partial X}\right)+2\frac{\partial H}{\partial \Phi}\right] \tag{13}$$

where X, Y, P, H, and Φ are defined by $X=x/L_x$, $Y=y/L_y$, $H=h/\kappa$, $P=p/p_0$, and $\Phi=\varphi/\varphi_0$; $\chi=L_y/L_x$; $\Gamma=6\eta L_y^2/\varphi_0 p_0\kappa^2$; $\varphi_s=1.126\times10^{-0.25^{\,h/\varsigma}}$ with $h/\varsigma>5$ and $\varphi_s=1.899(h/\varsigma)^{0.89}\times10^{-0.92h/\varsigma+0.05(h/\varsigma)\times(h/\varsigma)}$ with $h/\varsigma\le5$; $\varphi_x=\varphi_y=1-0.9\times10^{-0.56h/\varsigma}$; ς and p_0 are the random roughness of the crankpin bearing surfaces and atmospheric pressure, respectively.

To solve equation (13) in the lubrication model of engine's crankpin bearing using partial textures, some assumptions are given as follows:

1 The pressure of the oil film in the crankpin bearing at inlet and outlet has been defined by p_0 and it is also the pressure at the boundaries $\{m, n, p, q\}$ of crankpin bearing in the same Figure 1(b).

2 The thickness of the oil film always exists on all over the bearing and crankpin's surfaces.

3 The maximum thickness of the oil film of crankpin bearing at $\{m, n\}$ has been defined as inlet and outlet values.

4 In the cavitation region of crankpin bearing, the pressure of the oil film is determined by $p_c=p_s$ with $p\le p_s$ and $p_c=p$ with $p>p_s$. Here, p_s is the saturation pressure of oil film.

Therefore, boundary pressure conditions of oil film in engine's crankpin bearing are provided as:

$$p_{(x=0)}=p_{(x=L_x)}\ \text{ and }\ p_{(y=0)}=p_{(y=L_y)}=0 \tag{14}$$

With the initial and boundary conditions of the pressure and thickness of oil film defined, both the thickness and pressure of the oil film in crankpin bearing could be determined through the simulation process of equation (13).

2.3 The assessment indicators of lubrication efficiency

When engine's crankpin bearing is working, to ensure the crankpin bearing works normally, the load bearing capacity (F_b) created by the pressure of oil film on the bearing area must balance with the dynamics load F_c impacting on engine's crankpin bearing ($F_b = F_c$). Here, the F_b in the engine's crankpin bearing was expressed as follows (Nguyen et al., 2021):

$$F_b = \sqrt{(\iint_S \sin\psi(p + p_{ac})\mathrm{d}x\mathrm{d}y)^2 + (\iint_S \cos\psi(p + p_{ac})\mathrm{d}x\mathrm{d}y)^2} \tag{15}$$

where p_{ac} is the asperity pressure generated at the mixed-lubrication region of crankpin bearing.

Additionally, the friction force of the crankpin bearing has been also computed by (Patir and Cheng, 1979):

$$F_f = \iint_S (\tau + \tau_{ac})\mathrm{d}x\mathrm{d}y \tag{16}$$

where τ and τ_{ac} are the stress of the interfacial shear and asperity contact of two surfaces of crankpin bearing.

From equations (15) and (16), the load-bearing capacity and friction force are determined based on the thickness and pressure of oil film. Besides, both these parameters also greatly affect the journal bearings' lubrication (Papadopoulos et al., 2011). Therefore, in order to ameliorate the lubrication in an engine, the friction of the crankpin bearing needs to be reduced while its load-bearing capacity needs to be increased. To solve these issues, the different structures of partial textures with their optimal parameters are added to bearing surface to enhance both the thickness and pressure of the oil film. To assess engine's lubrication with crankpin bearing designed and added by the partial textures, the pressure and friction of oil film in crankpin bearing have been used as objective function.

3 Numerical simulation and result analysis

In order to calculate the oil film thickness, oil film pressure, and friction force of an engine's crankpin bearing impacted by the dynamic load (F_c) at 2×10^3 rpm in Figure 3 (Nguyen et al., 2021), based on design parameters of the crankpin bearing and partial textures given in Table 1 (Zhang et al., 2022; Ni et al., 2022), the engine's lubrication is then simulated and calculated via an algorithm program described and given in Figure 4 with "Calculation diagram". The computation steps are performed as following:

Step 1: Initial coefficients of partial textures, crankpin bearing as well as input data of the dynamics load F_c are defined as input values. Then, the friction force's vector ($1\times y = 1\times120$), matrix of the stress and pressure of oil film ($x\times y = 120\times120$), and matrix of the partial textures ($a\times b = 4\times6$) are established in MATLAB software. Based on the initial boundaries of the crankpin bearing, both the initial values of the stress and pressure of the oil film are then computed, respectively.

Table 1 Design parameters of an engine's crankpin bearing and partial textures

Parameters	*Values*	*Parameters*	*Values*	*Parameters*	*Values*
L_x (m)	126×10^{-3}	R (m)	0.8×10^{-3}	l_t (m)	1.6×10^{-3}
L_y (m)	18×10^{-3}	R_b (m)	20.08×10^{-3}	κ(m)	24.40×10^{-6}
h_{textures} (m)	5.5×10^{-6}	ς(m)	3.56×10^{-6}	δ(°)	65

Figure 3 Impacting force of f_c on an engine's crankpin bearing (see online version for colours)

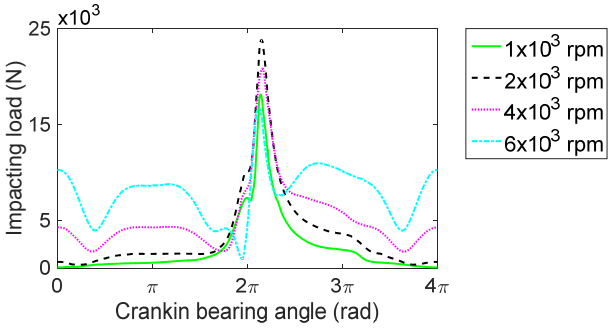

Figure 4 Calculation diagram of the crankpin bearing and optimisation algorithm of the micro-textures (see online version for colours)

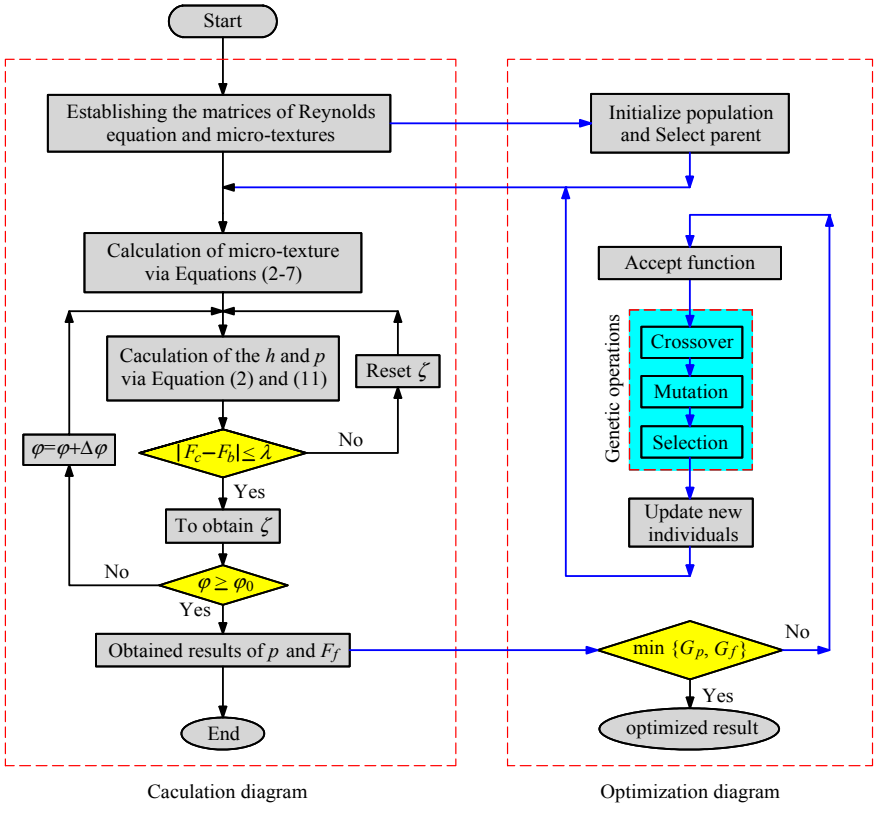

Step 2: From the initial results of the stresses and pressure of oil film calculated, the initial load-bearing capacity (F_b) generated by the pressure of oil film on the bearing area is then computed; and the value of the F_b balance with the dynamic load ($F_b = F_c$) to ensure the crankpin bearing works normally. However, it is difficult to reach the values of $F_b = F_c$ in the actual condition of the crankpin bearing working. The result is $F_b \neq F_c$. Therefore, the algorithm's stop condition is very difficult to achieve with $F_b = F_c$. To obtain this stop condition, a small error between F_b and F_c is then established by $\zeta = 0.001$. If the $|F_c - F_b| \leq \zeta$ then both values of the F_b and F_c are defined by $F_b = F_c$ the algorithm program is terminated. Then, both the results of the thickness and pressure of oil film are accepted. Conversely, the oil film thickness is changed until $|W_c - F_b| \leq \zeta$ obtained.

Step 3: The rotation angle in a working cycle of crankpin bearing is $\varphi_0 = 4\pi$ rad and divided by 120 equal parts with each note of $\Delta\varphi = 0.1\pi$ rad to compute both thickness and pressure of oil film at each rotation angle φ. Then, the next loop of the calculation program at $\varphi = \varphi + \Delta\varphi$ has been computed until $\varphi \geq \varphi_0$ to determine the oil film thickness, pressure, load bearing capacity, and friction force of the engine's crankpin bearing. Through the algorithm program and calculation result, the lubrication performance in an engine's crankpin bearing added by different textures is analysed.

3.1 Effect of different structures of partial textures

From design parameters of an engine's crankpin bearing listed in Table 1, the depth and dimensions of all different textures of $h_{textures} = 5.5\times10^{-6}$ m and $l_t = 2R = 1.6\times10^{-3}$ m, and matrix of partial textures ($a\times b = 4\times6$), the depth and shape's distribution in all spherical textures (ST), CCT, conical textures (CT), CST, WST, and full textures are plotted in Figure 5(a)–(f). Concurrently, the pressure distribution of the oil film in crankpin bearing with ST, CCT, CT, SCT, WST, and full textures is also shown in Figure 6(a)–(f), respectively.

The results in Figure 6(a)–(f) show that under the different shapes and depths the partial textures designed on bearing surface, the maximum pressure of oil film with ST(4×6), CCT(4×6), CT(4×6), SCT(4×6), WST(4×6), and full textures is obtained at 229×10^6, 225×10^6, 227×10^6, 224×10^6, 226×10^6, and 219×10^6 Pa, respectively. In addition, the maximum pressure of oil film in crankpin bearing using ST(4×6) is increased compared to all different textures of CCT(4×6), CT(4×6), SCT(4× 6), WST(4×6), and full texture. This obtained result could be due to the effect of dimension parameters of the various partial textures. With the structure of both CCT(4×6) and SCT(4×6) used, their structures in Figure 5(b)–(d) show that their depth (or oil film thickness) are unchanged. Thereby, the cavitation pressure of the thickness of oil film is increased and maximum pressure of oil film is significantly reduced. With the structures of ST(4×6), CT(4×6), and WST(4×6) applied, their structures in Figure 5(a), (c) and (e) show that their depth (or thickness of oil film) is significantly unchanged. The result is the cavitation pressure of oil film thickness is lightly increased, so the maximum pressure of oil film has been increased, especially with the bearing surface added by ST(4×6). Thus, the lubrication performance of the spherical textures is better than the different partial textures. This result was also performed in the research of Papadopoulos et al. (2011) on the journal bearings. In the study of Nguyen et al. (2021), the maximum pressure of oil film in an engine's crankpin bearing using ST(4×6) was also increased by

4.8% compared to full textures in Figure 6(f). Consequently, compared to using full textures, ST(4×6) also better improves the engine's lubrication.

Figure 5 Distribution of the different textures in an engine's bearing surface: (a) ST(4×6); (b) CCT(4×6); (c) CT(4×6); (d) SCT(4×6); (e) WST(4×6) and (f) full textures (see online version for colours)

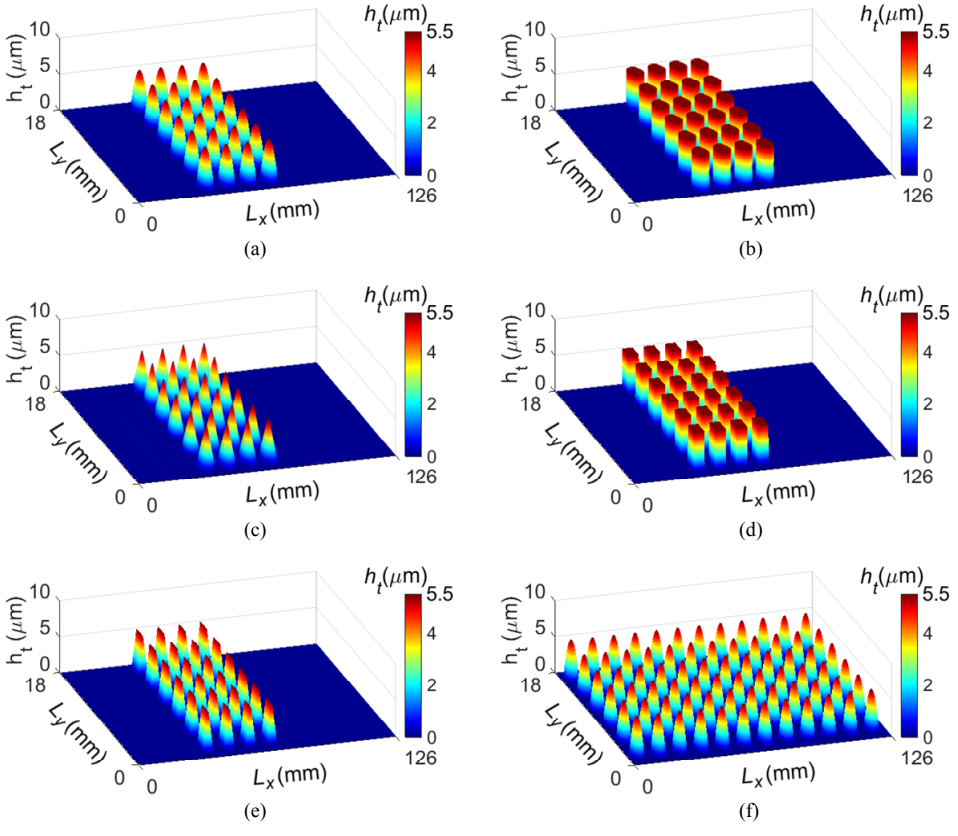

From the simulation result of the pressure and stress of oil film with different partial textures, the friction force and maximum friction force in an engine's crankpin bearing have been plotted in Figures 7 and 8. Observing both Figures 7 and 8, the friction force and maximum friction force of crankpin bearing designed by ST(4×6) are remarkably reduced in comparison with CCT(4×6), CT(4×6), SCT(4×6), WST(4×6), and full textures. Particularly, the maximum friction force in an engine's crankpin bearing using ST(4×6) is decreased by 10.6% in comparison with full textures applied on all bearing surfaces. Thereby, by designing ST(4×6) on the bearing surface of crankpin bearing at its mixed lubrication region, the lubrication of an engine's crankpin bearing could be better than using other structures of the partial textures. However, only the structure of partial textures with the distribution density of (a×b = 4×6) is simulated and assessed. The existing research noted that the lubrication in journal bearings had been also affected by the distribution density of micro-textures (Nguyen et al., 2021; Zhang et al., 2022). Therefore, the density effect of spherical textures on the lubrication of an engine is also evaluated in the next section.

Figure 6 Influence of the different textures on the pressure of the oil film: (a) ST(4×6); (b) CCT(4×6); (c) CT(4×6); (d) SCT(4×6); (e) WST(4×6) and (f) full textures (see online version for colours)

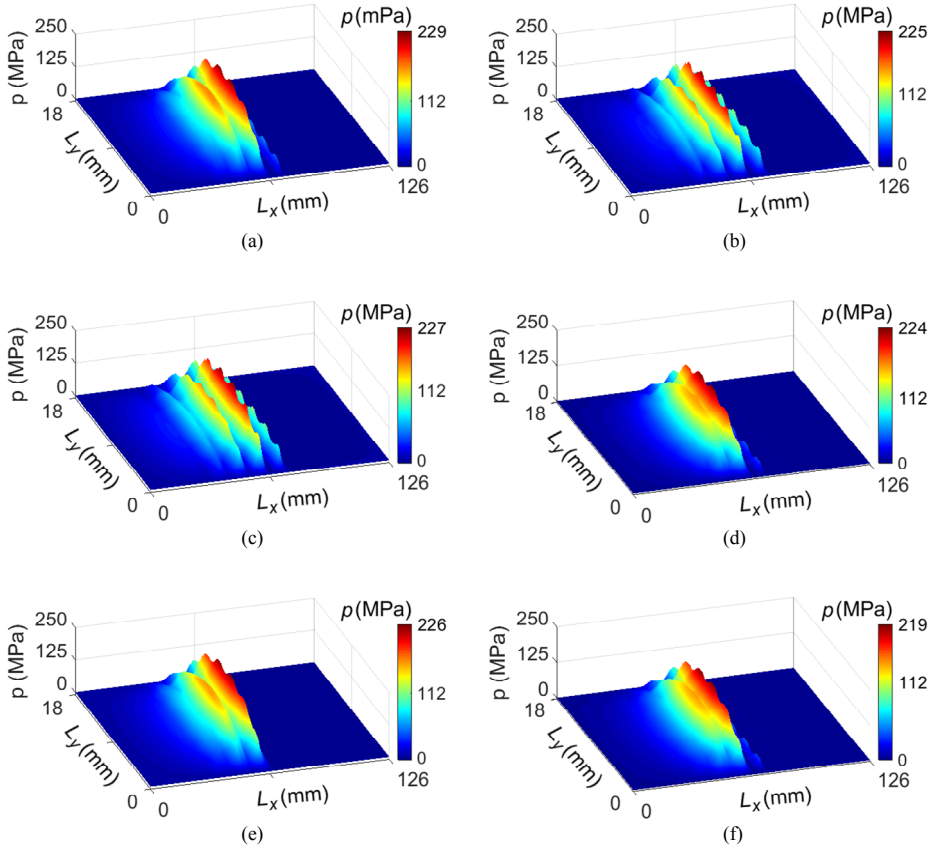

Figure 7 Effect of different textures on an engine's friction force (see online version for colours)

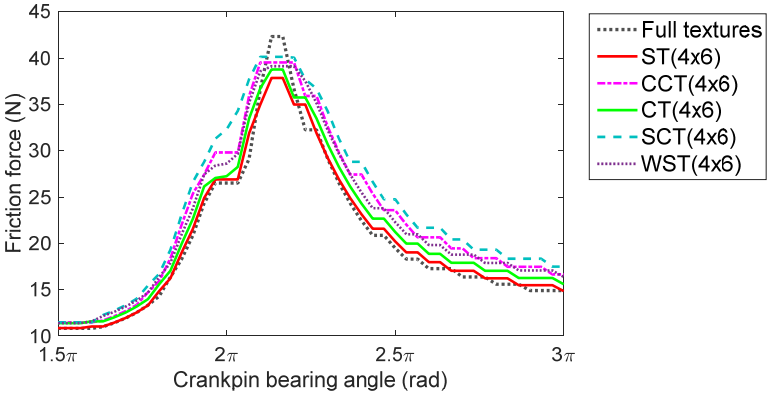

Figure 8 Maximum friction force of crankpin bearing obtained with different textures (see online version for colours)

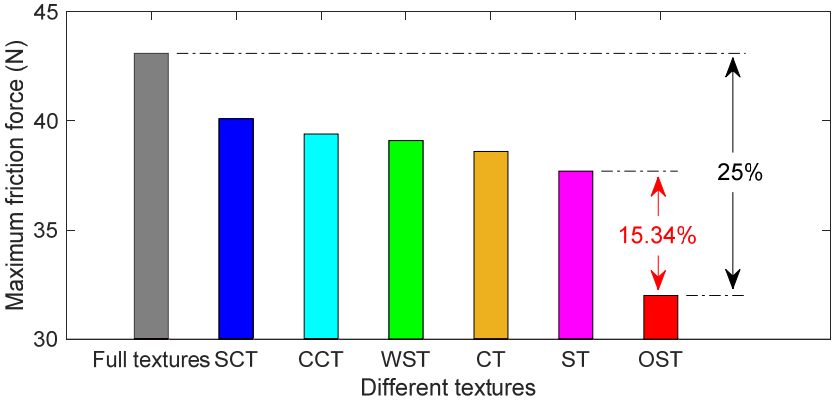

3.2 Distribution effect of spherical textures on bearing surface

Three various densities of spherical textures such as ST(3×6), ST(4×6), and ST(5×6) have been simulated and computed for the friction and lubrication of an engine. From the simulation result, both the density and pressure of oil film in engine's bearing surface designed by ST(3×6), ST(4×6), and ST(5×6) are plotted in Figures 9(a)–(c) and 10(a)–(c).

Figure 9 Distribution density of spherical textures on an engine's bearing surface: (a) ST(3×6); (b) ST(4×6) and (c) ST(5×6) (see online version for colours)

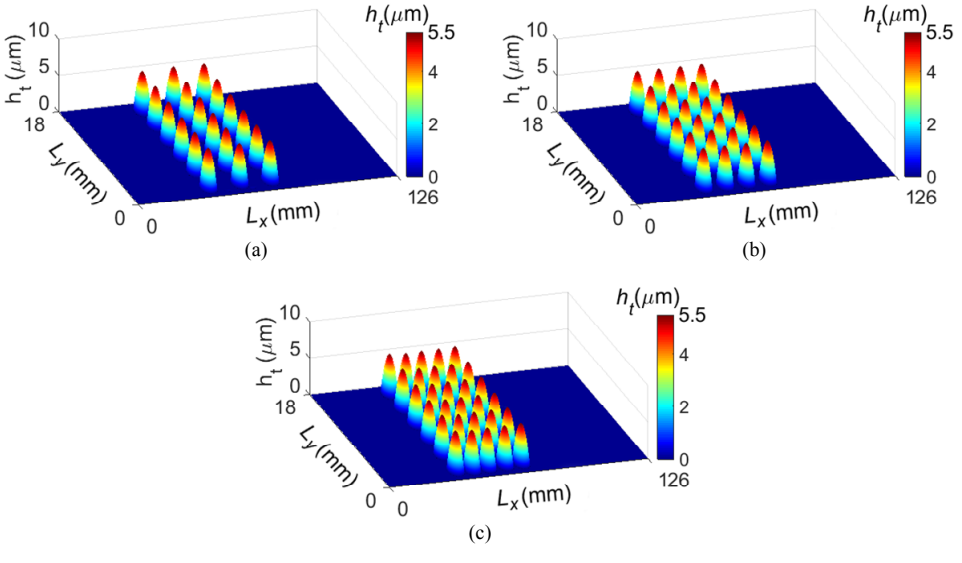

Figure 10 Effect of the density of spherical textures on the oil film pressure: (a) ST(3×6); (b) ST(4×6) and (c) ST(5×6) (see online version for colours)

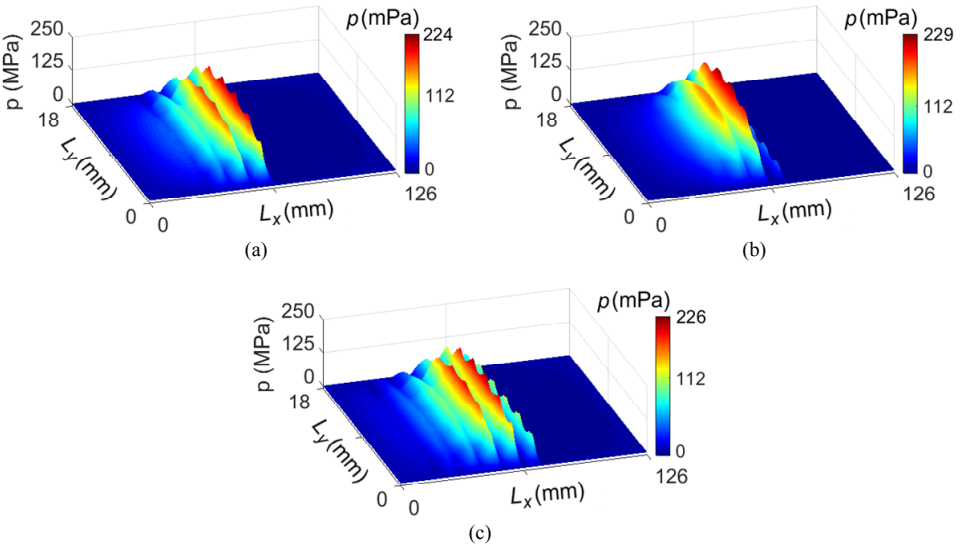

Figure 10(a)–(c) show that the maximum pressure of oil film in engine's crankpin bearing designed by ST(3×6) and ST(5×6) is significantly reduced compared to ST(4×6). This implies that the lubrication of the engine's crankpin bearing using ST(4×6) is improved better than ST(3×6) and ST(5×6). This result is also similar to the result in the research of Nguyen et al. (2021). From the simulation result of the stress and pressure of the oil film using various densities of spherical textures, the friction force of the engine's crankpin bearing is also shown in Figure 11.

Figure 11 Effect of the density of spherical textures on an engine's friction force (see online version for colours)

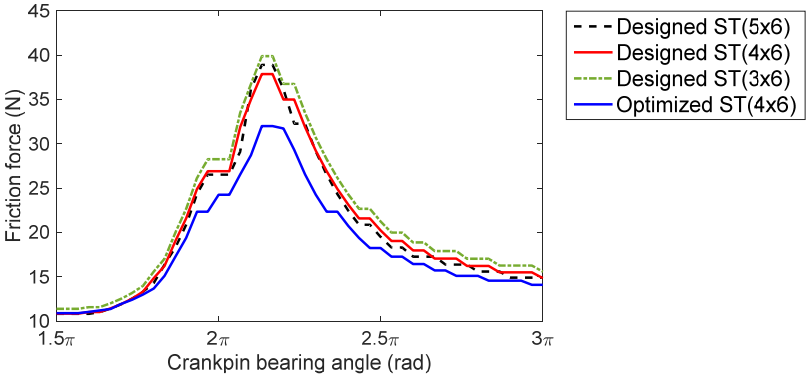

Figure 11 shows that the friction force of engine's crankpin bearing is insignificantly changed by three different densities of the spherical textures. However, the maximum friction of the crankpin bearing designed by the ST(3×6) and ST(5×6) are significantly reduced in comparison with the ST(4×6). This means that the increase or reduction of the

density of spherical textures could affect the lubrication performance of an engine's crankpin bearing using spherical textures. Therefore, the density of ST(4×6) should be applied for designing the partial textures on engine's crankpin bearing. Besides, the existing research noted that the lubrication in journal bearings had been affected by different parameters of the depths and radios in each micro-texture (Guzek et al., 2013; Kim et al., 2014). However, in this study, the radius (R) and depth ($h_{textures}$) of all the spherical textures are similar and unchanged. Therefore, the design parameters of each texture (i, j) of the ST(4×6) including the $R(i, j)$ and $h_{textures}(i, j)$ should be also optimised to enhance the engine's lubrication. This issue will be done in the next section.

4 Optimisation of design parameters of spherical textures

4.1 Multi-objective optimum algorithm

The genetic algorithm was an optimal algorithm to find the minimum value or maximum value based on input values. A genetic algorithm was expressed as follows (Zhang et al., 2022; Jain and Parashar, 2022):

Search a vector of $\boldsymbol{g} = [g_1, g_2, g_3,..., g_n]^T$ to optimum

$$\boldsymbol{G}(\boldsymbol{g}) = [G_1(\boldsymbol{g}), G_2(\boldsymbol{g}), G_3(\boldsymbol{g}),..., G_n(\boldsymbol{g})]^T \quad (20)$$

s.t. $G_i(g) \le 0$ $n = 1, 2,..., N$

$H_j(g) = 0$ $m = 1, 2,..., M$

where $\boldsymbol{G}(\boldsymbol{g})$ is the optimal objective; N and M are the number in the equality constraint and inequality constraint.

In order to obtain the maximum pressure of oil film and minimum friction force of the crankpin bearing with the ST(4×6), the design parameters of the $R(i, j)$ and $h_{textures}(i, j)$ of each spherical texture are then optimised via genetic algorithm. From initial parameters of spherical textures ($R = 0.8\times10^3$ m and $h_{textures} = 5.5\times10^{-6}$ m), these parameters are then encoded and connected to the chromosome of $\boldsymbol{g} = [R, h_{textures}]^T$. Here $R = [R(1,1), R(1,2), ..., R(i, j), ..., R(4,6)]^T$ and $h_{textures} = [h_{textures}(1,1), h_{textures}(1,2), ..., h_{textures}(i, j), ..., h_{textures}(4,6)]^T$, ($0.2\times10^{-3} \le R(i, j) \le 4.0\times10^{-3}$ m and $0.1\times10^{-6} \le h_{textures}(i, j) \le 10\times10^{-6}$ m). In order to search the maximum pressure of oil film and minimum friction force of engine's crankpin bearing, two objective functions are then defined for the optimisation process:

$$G_p = \text{maximum}\ \{p_{\max}(i, j)\} \ \text{ and } \ G_f = \text{minimum}\ \{F_{f\max}(i, j)\} \quad (21)$$

Via the computation process of the lubrication model of the engine's crankpin bearing using ST(4×6) in the same Figure 4 with "Optimisation diagram", the obtained results of the higher value of G_p and lower value of G_f with parameters of $R(i, j)$ and $h_{textures}(i, j)$ indicate that values of $R(i, j)$ and $h_{textures}(i, j)$ are very good. These values are then updated and optimised in 10^3 generation (g).

4.2 Analysis of the lubrication performance of optimised spherical textures

From the initial parameters of spherical textures and crankpin bearing provided in Table 1, the radius and depth of each spherical texture $R(i, j)$ and $h_{textures}(i, j)$ have been

optimumed through the genetic algorithm described and given in the same Figure 4 with "Optimisation diagram". The obtained fitness values of the maximum pressure of the oil film (G_p) and minimum friction force (G_f) are then saved and shown in Figure 12(a) and (b). Both Figure 12(a) and (b) show that the value of G_p is strongly increased from 0 to 390 while the value of G_f is strongly reduced from 0 to 376 of the evolutionary generations. Both the fitness values of G_p and G_f are insignificantly changed from 908 and 862 to the end of the generation. This means that optimal parameters of $R(i, j)$ and $h_{textures}(i, j)$ of the spherical textures could be obtained at 908 of the generation. These optimal parameters are then simulated and computed the optimal thickness and optimal pressure of the oil film in an engine's crankpin bearing. Both these optimal results have been plotted in Figure 13(a) and (b).

Figure 12 The fitness values of the optimised spherical textures: (a) the fitness value g_p and (b) fitness value g_f (see online version for colours)

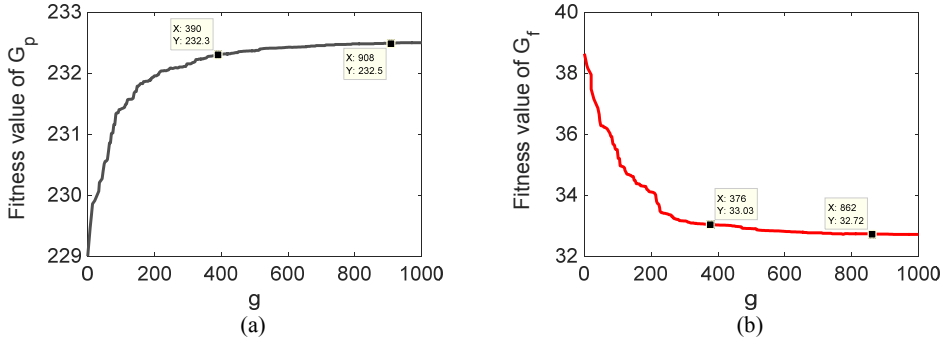

Figure 13 Results of h and p of the crankpin bearing using optimised ST(4×6): (a) the thickness of oil film and (b) pressure of oil film (see online version for colours)

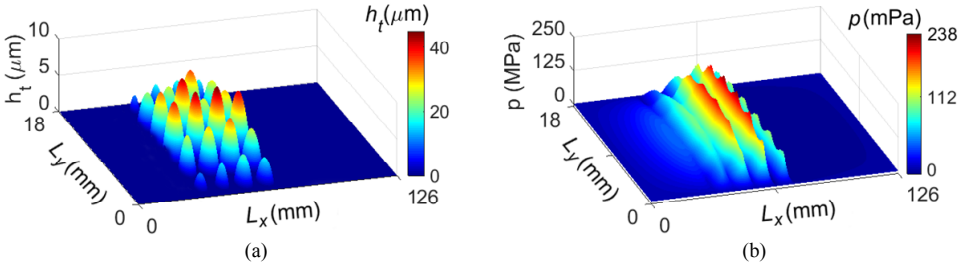

Figure 13(a) and (b) show that the pressure and thickness of oil film using optimised ST(4×6) are strongly increased at the centre region of the partial textures. Concurrently, the maximum values of the thickness and pressure of oil film are obtained at the centre region of the optimised ST(4×6). At the boundaries p and q of the crankpin bearing, the radius and depth of the optimised ST(4×6) in Figure 13(a) are smaller than that of the designed ST(4×6) in Figure 5(a). This means that the radios and depth at the centre region of spherical textures need to be ameliorated to obtain both the maximum thickness and maximum pressures of oil film. The result in Figure 13(b) shows that the maximum pressure of oil film in an engine's crankpin bearing designed by the optimised ST(4×6) is obtained by 238×10^6 Pa and this value is increased by 3.4% and 8.0% in comparison with

the crankpin bearing using the designed ST(4×6) and full textures. This implies that the optimised ST(4×6) could improve the lubrication of the engine better than the designed ST(4×6) and full textures.

From the pressure and stress of oil film computed with the optimised ST(4×6), the maximum friction force and friction force in an engine's crankpin bearing using optimised ST(4×6) are also computed and compared in the same Figures 8 and 11. The result indicates that the friction force in crankpin bearing with optimised ST(4×6) is obviously decreased compared to all different distribution densities of the ST(3×6), ST(4×6), and ST(5×6) (see Figure 11). Especially, the maximum friction of the engine's crankpin bearing with optimised ST(4×6) is increased by 15.34% and 25% compared to designed ST(4×6) and full textures (see Figure 8). This is due to the increase in the radius, depth, and maximum pressure of oil film at the central region of the optimised ST(4×6). The result is the reduction of solid asperity contacts between the bearing and crankpin surface at the mixed lubrication region of the crankpin bearing. Thereby, the crankpin bearing's friction force is also reduced and the lubrication of the engine is ameliorated.

4.3 Analysing the performance of spherical textures optimised under engine speeds

When the engine is working, its load and angular speed are always changed. Therefore, three different loads and angular speeds of 10^3 rpm, 4×10^3 rpm, and 6×10^3 rpm of the engine in the same Figure 3 are also simulated to fully assess the performance of optimised ST(4×6) for reducing the friction force of an engine. Both friction and maximum friction forces of the engine's crankpin bearing using optimised ST(4×6) have been shown in Figure 14 and provided in Table 2.

Table 2 The maximum friction force in the engine's crankpin bearing using with and without optimisation of the spherical textures

CB's angular speed (rpm)	*Maximum friction force (N)*		
	Designed ST	*Optimised ST*	*Reduction (%)*
1×10^3 (rpm)	37.34	30.10	19.38
4×10^3 (rpm)	51.39	45.28	11.88
6×10^3 (rpm)	54.26	50.08	7.70

Figure 14 also indicates that the friction force of the crankpin bearing using the optimised ST(4×6) is smaller than that of the designed ST(4×6) under the engine's various speeds. Especially, the comparison results of the maximum friction force in Table 2 show that the maximum friction force of the crankpin bearing using the optimised ST(4×6) at 1×10^3 rpm, 4×10^3 rpm, and 6×10^3 rpm is reduced by 19.38%, 11.88%, and 7.70% in compared to the designed ST(4×6), respectively. This result implies that under the different loads and speeds of an engine, both engine's lubrication and friction are improved by using optimised ST(4×6), especially at the low speeds of 10^3 rpm and 2×10^3 rpm of the engine. Thus, to reduce friction and enhance the durability of the

engine, the working speed range of the engine from 10^3 rpm to 2×10^3 rpm should be maintained.

Figure 14 Friction force of engine's crankpin bearing using the spherical textures with and without optimisation: (a) at 10^3 rpm; (b) at 4×10^3 rpm and (c) at 6×10^3 rpm of the engine (see online version for colours)

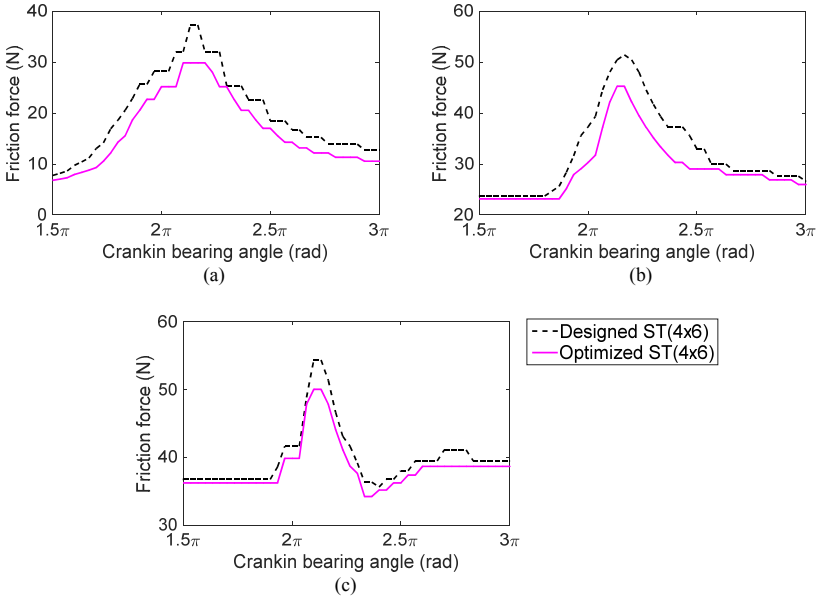

5 Conclusion

By designing and adding the partial textures on an engine's crankpin bearing, an engine's lubrication performance is significantly ameliorated compared to full textures designed on engine's crankpin bearing.

With different structures of ST(4×6), CCT(4×6), CT(4×6), SCT(4×6), and WST(4×6) simulated and analysed, the result of ST(4×6) better improves engine's lubrication in comparison with other partial textures. Besides, the density of ST(4×6) distributed on the bearing surface also better improves engine's lubrication compared to both distribution densities of ST(3×6) and ST(5×6). Thus, the bearing surface should be added by ST(4×6) for improving the lubrication in engine.

With the radius and depth of ST(4×6) optimised, the maximum pressure of oil film and maximum friction force in engine's crankpin bearing are obviously improved by 8% and 25% compared to full textures designed on crankpin bearing's bearing surface. Therefore, in order to further ameliorate the lubrication performance as well as enhance the durability of the engine, the optimised ST(4×6) should be applied to the crankpin bearing's bearing surface.

References

Arulbrittoraj, A., Gurumoorthy, A., Karthikeyan, S. and Duraiselvam, M. (2020) 'Study the effect of roller hardness on the surface properties of burnished AISI 1211 steel', *International Journal of Computational Materials Science and Surface Engineering (IJCMSSE)*, Vol. 9, No. 1, pp.53–69.

Bolutife, O., Cinta, L., Oyelayo, O. and Ezekiel, O. (2015) 'Effect of laser surface texturing (LST) on tribochemical films dynamics and friction and wear performance', *Wear*, Vols. 332–333, No. 1, pp.1225–1230.

Dobrica, M., Fillon, M., Pascovici, M. and Cicone, T. (2010) 'Optimizing surface texture for hydrodynamic lubricated contacts using a mass-conserving numerical approach', *Proc. IMechE, Part J: Journal of Engineering Tribology*, Vol. 224, No. 8, pp.737–750.

Fouflias, D., Charitopoulos, A., Papadopoulos, C. and Kaiktsis, L. (2017) 'Thermohydrodynamic analysis and tribological optimization of a curved pocket thrust bearing', *Tribology International*, Vol. 110, No. 1, pp.291–306.

Guzek, A., Podsiadlo, P. and Stachowiak, G. (2013) 'Optimization of textured surface in 2D parallel bearings governed by the Reynolds equation including cavitation and temperature', *Tribology Online*, Vol. 8, No. 1, pp.7–21.

Hua, W., Nguyen, V. and Jiao, R. (2022) 'Investigation of distribution and structure of surface textures on improving tribological properties of an engine', *SAE International Journal of Engines*, Vol. 15, No. 3, pp.381–392.

Jain, S. and Parashar, V. (2022) 'Optimisation of EDM process parameters: by butterfly optimisation algorithm and genetic algorithm', *International Journal of Computational Materials Science and Surface Engineering (IJCMSSE)*, Vol. 11, No. 1, pp.21–46.

Kim, B., Chae, Y. and Choi, H. (2014) 'Effects of surface texturing on the frictional behavior of cast iron surfaces' *Tribology International*, Vo. 70, No. 1, pp.128–135.

Liu, S. and Ye, H. (2021) 'Improving the tensile and fatigue crack growth properties of SLM Ti-6Al-4V alloy by heat treatment and ultrasonic surface rolling process', *International Journal of Computational Materials Science and Surface Engineering (IJCMSSE)*, Vol. 10, Nos. 3–4, pp.149–164.

Michalec, M., Svoboda, P., Křupka, I. and Hartl, M. (2021) 'A review of the design and optimization of large-scale hydrostatic bearing systems', *Engineering Science and Technology, an International Journal*, Vol. 24, No. 4, pp.936–958.

Mourier, L., Mazuyer, D., Ninove, F. and Lubrecht, A. (2010) 'Lubrication mechanisms with laser-surface-textured surfaces in elastohydrodynamic regime', *Proc. IMechE, Part J: Journal of Engineering Tribology*, Vol. 224, No. 8, pp.697–711.

Nguyen, V., Zhang, J. and Huang, D. (2021) 'Influence of micro asperity contact and radial clearance on the tribological properties of crankpin bearings', *Journal of Southeast University*, Vol. 37, No. 3, pp.264–271.

Nguyen, V., Zhang, J. and Jiao, R. (2021) 'Method of ameliorating the lubrication and friction performance of an engine based on different microtextures', *Journal of Southeast University*, Vol. 37, No. 4, pp.365–371.

Ni, D., Nguyen, V. and Huan, Y. (2022) 'Improving the engine lubrication and friction with spherical dimples of partial textures optimized on crankpin bearing surface', *SAE Int. J. Fuels and Lubricants*, Vol. 15, No. 3, pp.743–754.

Papadopoulos, C., Efstathiou, E., Nikolakopoulos, P. and Kaiktsis, L. (2011) 'Geometry optimization of textured three-dimensional micro-thrust bearings', *Journal Tribology*, Vol. 133, No. 4, pp.041702.

Patir, N. and Cheng, H. (1978) 'An average flow model for determining effects of three-dimensional roughness on partial hydrodynamic lubrication', *Journal of Lubrication Technology*, Vol. 100, No. 1, pp.12–17.

Patir, N. and Cheng, H. (1979) 'Application of average flow model to lubrication between rough sliding surfaces', *Journal of Lubrication Technology*, Vol. 101, No. 2, pp.220–229.

Shen, C. and Khonsari, M. (2015) 'Numerical optimization of texture shape for parallel surfaces under unidirectional and bidirectional sliding', *Tribology International*, Vol. 82, Part A, pp.1–11.

Sinanoğlu, C., Nair, F. and Karamış, M. (2005) 'Effects of shaft surface texture on journal bearing pressure distribution', *Journal of Materials Processing Technology*, Vol. 168, No. 2, pp.344–353.

Wang, P., Nguyen, V., Wu, X. and Wang, S. (2021) 'Research on different structures of dimpled textures on improving the LE-FPL of engine', *Industrial Lubrication and Tribology*, Vol. 73, No. 4, pp.545–553.

Xu, S., Nguyen, V., Wang, X. and Zhou, H. (2022) 'Sensitivity analysis of the geometrical dimensions of the crankpin bearing on the tribological property of an engine', *SAE International Journal of Engines*, Vol. 15, No. 3, pp.367–380.

Zhang, B., Ren, G., Nguyen, V., Wang, Y. and Xu, C. (2022) 'Optimizing the parameters of the partial textures of the crankpin bearing to enhance the lubrication performance of an engine', *SAE International Journal of Engines*, Vol. 15, No. 5, pp.743–754.